

Virus Trap in Human Serum Albumin Nanotube

Teruyuki Komatsu,^{*,†} Xue Qu,[‡] Hiromi Ihara,[§] Mitsuhiro Fujihara,[§] Hiroshi Azuma,[§] and Hisami Ikeda[§]

[†]Department of Applied Chemistry, Faculty of Science and Engineering, Chuo University, 1-13-27 Kasuga, Bunkyo-ku, Tokyo 112-8551, Japan

[‡]Research Institute for Science and Engineering, Waseda University, 3-4-1 Okubo, Shinjuku-ku, Tokyo 169-8555, Japan

[§]Hokkaido Red Cross Blood Center, 2-2 Yamanote, Nishi-ku, Sapporo-shi, Hokkaido 063-0002, Japan

S Supporting Information

ABSTRACT: Infectious hepatitis B virus (HBV), namely Dane particles (DPs), consists of a core nucleocapsid including genome DNA covered with an envelope of hepatitis B surface antigen (HBsAg). We report the synthesis, structure, and HBV-trapping capability of multilayered protein nanotubes having an anti-HBsAg antibody (HBsAb) layer as an internal wall. The nanotubes were prepared using an alternating layer-by-layer assembly of human serum albumin (HSA) and oppositely charged poly-L-arginine (PLA) into a nanoporous polycarbonate (PC) membrane (pore size, 400 nm), followed by depositions of poly-L-glutamic acid (PLG) and HBsAb. Subsequent dissolution of the PC template yielded (PLA/HSA)₂PLA/PLG/HBsAb nanotubes (AbNTs). The SEM measurements revealed the formation of uniform hollow cylinders with a 414 ± 16 nm outer diameter and 59 ± 4 nm wall thickness. In an aqueous medium, the swelled nanotubes captured noninfectious spherical small particles of HBsAg (SPs); the binding constant was 3.5 × 10⁷ M⁻¹. Surprisingly, the amount of genome DNA in the HBV solution (HBsAg-positive plasma or DP-rich solution) decreased dramatically after incubation with the AbNTs (−3.9 log order), which implies that the infectious DPs were completely entrapped into the one-dimensional pore space of the AbNTs.

Organic nanotubes have attracted great interest because of their potential applications for smart biological devices in aqueous media^{1–9} such as molecular flow channels,^{1c} drug delivery containers,^{3,4a,5,8,9} and cylindrical nanoreactors.^{4b,6b} Various guest molecules are selectively encapsulated into their one-dimensional pore space *via* capillary force,^{1a,b} electrostatic attraction,^{1c,5,8} and biospecific interaction.^{4a,5,9} One efficient procedure to prepare the structure-defined hollow cylinder is template synthesis using layer-by-layer (LbL) assembly in nanoporous membrane.^{4–10} We recently demonstrated that human serum albumin (HSA) nanotubes with an avidin surface interior can readily load biotin-labeled nanoparticles.⁹ This flexibility of function program by LbL buildup is stimulating efforts to create a nanotubular trap for infectious viruses using antigen–antibody reaction. Hepatitis B virus (HBV) is the major cause of liver disease. Despite the existence of vaccination, more than 300 million people are chronically infected with HBV worldwide.^{11,12}

Some patients fail to identify the virus, and 10–30% develop liver cirrhosis with possible progression to liver cancer.¹³ The intact and infectious HBV, the so-called Dane particle (DP, $r = 42$ nm), comprises a core nucleocapsid including partially double-stranded DNA covered with an envelope. The envelope consists of hepatitis B surface antigen (HBsAg, M_w : *ca.* 25 kDa), which individually self-organizes to generate a noninfectious spherical small particle (SP, $r = 22$ nm) and rod-like long particle (LP, $r = 22$ nm, $l = 50–700$ nm) (Figure 1a). They adsorb anti-HBsAg antibody (HBsAb) as a decoy to reduce the immune reaction.¹⁴ If one can create a unique nanotubular trap for the infectious DP, then it would have an important impact not only on bioseparation chemistry but also on medical applications. Nanotubes present several advantages over nanospheres.¹⁵ (i) Multifunctionalities can be introduced on the inner and outer surfaces independently. (ii) Open-end terminals enable quick loading of target molecules without structural change. (iii) Nanotubes can have long circulation persistence in the bloodstream.³ In this paper, we first describe the synthesis, structure, and HBV-trapping capability of HSA nanotubes having an HBsAb layer as an internal wall, and highlight that the infectious DPs are perfectly entrapped into the cylindrical pore.

The nanotubes were fabricated using electrostatic LbL assembly principles.⁹ Positively charged poly-L-arginine (PLA) and negatively charged HSA were alternately deposited (2.5 cycles) onto the channel surface of a track-etched polycarbonate (PC) membrane (pore size, 400 nm), followed by depositions of poly-L-glutamic acid (PLG) as the sixth layer and HBsAb (goat polyclonal antibody) as the last layer of the wall. Isoelectric focusing of HBsAb exhibited a *pI* value of 8–10. Therefore negatively charged PLG (an electrostatic glue) was sandwiched between the PLA and HBsAb layers. Dissolution of the PC template in *N,N*-dimethylformamide and subsequent freeze-drying of the extracted core yielded (PLA/HSA)₂PLA/PLG/HBsAb nanotubes (AbNTs) as a white powder. Later, SEM measurements revealed the formation of uniform hollow cylinders with an outer diameter of 414 ± 16 nm and wall thickness of 59 ± 4 nm (Figure 1b). The maximum length of the tubules (*ca.* 9 μm) corresponded to the channel depth of the PC membrane. TEM observations showed that the AbNTs swelled considerably in water, and their wall thickness became approximately double (109 ± 5 nm) that of the dried state (Figure 1c). The outer diameter was almost unaltered. Thereby the inner pore size diminished to *ca.* 200 nm.

Received: October 26, 2010

Published: February 22, 2011

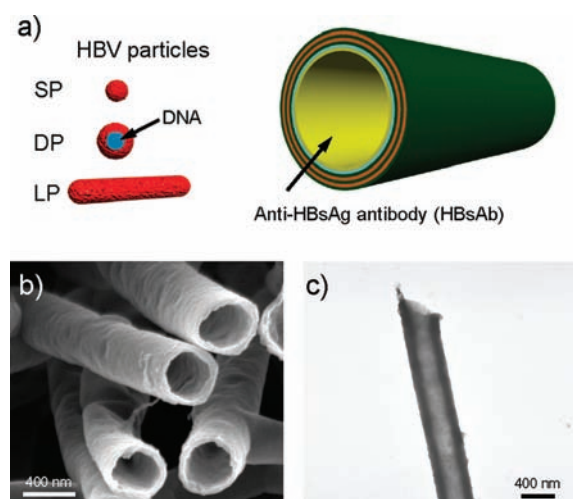


Figure 1. (a) Schematic illustrations of three types of HBV particles (SP, DP, LP) and (PLA/HSA)₂PLA/PLG/HBsAb nanotube (AbNT). (b) SEM image of lyophilized AbNTs prepared using porous PC template ($D_p = 400$ nm), and (c) TEM image of AbNT stained with uranylacetate.

The amount of HBsAb on the pore surface was estimated. The powder of AbNTs (*ca.* 210 μg) obtained from one PC membrane (diameter, 25 mm), in which *ca.* 3.0×10^8 channels exist, was dispersed in acidic water (pH 3.5, 1.5 mL) to dissolve the multilayered structure. From the absorbance at 280 nm, the HBsAb concentration was determined to be *ca.* 75 nM, under the assumption that the AbNTs consist of the LbL assembly described above. It became apparent that one AbNT (length, 9 μm) contains *ca.* 2.2×10^5 molecules of HBsAb.

We used three different HBV solutions (HBV1–3) for trap experiments: HBsAg SP solution (HBV1), HBsAg-positive plasma including all particles (SP, DP, and LP) (HBV2), and DP-rich solution (HBV3). Actually, SP, DP, and LP can all be detected by HBsAg assay; only DP is found by DNA assay. First, HBV1 (1 $\mu\text{g}/\text{mL}$, 7.5 μL) was added to the AbNT dispersion (pH 7.4, 0.75 mL) in phosphate buffered saline (PBS). To avoid an electrostatic attraction between the HBV particles and tube surface exterior, free HSA was added to the nanotube dispersion ([HSA] = 0.2 mM). After incubation for 3 h at room temperature, the mixture was centrifuged for 10 min at $5000 \times g$ to spin down the tubes. The HBV-trapping capability of the AbNT was determined using chemiluminescence enzyme immunoassay (CLEIA) of the remaining HBsAg in the supernatant. The amount of HBsAg was significantly lower than that of the identically treated HBV1 solution without the tubes (control group) (Figure 2a). The trapping ratio [$\{1 - \text{COI}(\text{AbNT})/\text{COI}(\text{Control})\} \times 100$] reached 90%. In contrast, incubation with the (PLA/HSA)₃PLA nanotubes (NTs) did not cause a marked difference in the HBsAg numbers. Chemiluminescence immunoassay (CLIA) yielded similar results (Figure S1). Remarkably, CLEIA and CLIA measurements were not reproducible for the PBS solution without 0.2 mM HSA. In SDS PAGE of the concentrated supernatant, no HBsAb band appeared between 130 and 150 kDa. This manifests that the AbNTs retain their original multilayered structure without the antibody release during the experiments. We concluded that the HBV SPs diffused into the hollow space of the AbNT and bind to the inner surface wall. The concentration dependence of the absorbed HBsAg (Figure S2)

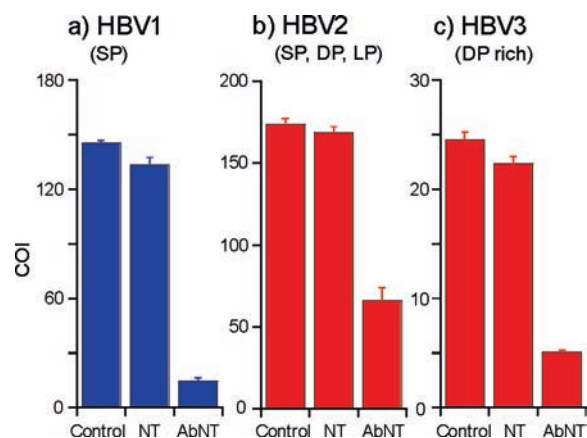


Figure 2. Amount of remaining HBsAg in HBV1–3 solutions (PBS, pH 7.4, 0.2 mM HSA) after incubation with AbNTs, with NTs, and without tubes (control) determined using the CLEIA method. The vertical axis is defined as the cutoff index (COI).

Table 1. Amount of Remaining DNA in HBV2 and HBV3 Solutions (PBS, pH 7.4, 0.2 mM HSA) after Incubation with AbNTs

[DNA] (copies/mL)	HBV2	HBV3
Control (without tubes)	1.23×10^5	2.58×10^5
AbNT	166	36
Trapping ratio (%)	99.87	99.99

conferred a binding constant (K) of $3.5 \times 10^7 \text{ M}^{-1}$. Generally, the K value of the antigen–antibody reaction is between 10^8 and 10^9 M^{-1} . The low binding affinity of HBsAg (SP) to the AbNT appears to be attributable to the fact that some HBsAbs are adhered to the pore wall with unfavorable geometries, in which the antigen-binding fragments do not direct to the hollow center.

Next, we performed the same experiments using more practical HBV2 and HBV3 solutions. After incubation with the AbNTs for 3 h, the mixture was centrifuged to precipitate the tubes. The CLEIA of the supernatants demonstrated that the HBsAg-trapping ratio was, respectively, 62% for HBV2 and 79% for HBV3 (Figure 2b, c); these values are lower than that observed in the case of HBV1. At least two plausible reasons exist. First, HBV2 and HBV3 include certain amounts of LPs that are too large to enter the pore (*ca.* 200 nm). Second, a nonspecific antibody reaction takes place, because HBV2 and HBV3 are prepared from the HBsAg-positive plasma. The soluble inhibitor is likely to contribute the reduction of trap competence.

To evaluate the DP-trapping capability of the AbNT, DNA quantification assays of the supernatants were conducted by PCR. As presented in Figure 2b and 2c (control groups), the amount of HBsAg in the HBV3 solution was one-seventh of that of the HBV2 solution. Strikingly however, the DNA concentration in HBV3 (2.58×10^5 copies/mL) was 2-fold greater than that of HBV2 (Table 1). Therefore, HBV3 contains large quantities of infectious DPs. To our surprise, the DNA concentrations declined dramatically after incubation with the AbNTs: 166 copies/mL for HBV2 (trapping ratio, 99.87%) and 36 copies/mL for HBV3 (trapping ratio, 99.99%). We reasoned that DPs were entirely captured into the one-dimensional pore space of the AbNT, although noninfectious SPs and LPs still

existed in the bulk solution. TEM observation demonstrated the entrapping of DPs into the hollow (Figure S3). Results show that the AbNT treated HBV specimens became clinically DP free. The detailed supramolecular mechanism responsible for this perfect DP trapping into the AbNT remains unclear. Nevertheless, we presume that (i) dense and robust DP with genome DNA is favorable to bind to the pore wall of the cylinder or (ii) the large DP can possess multiple binding sites per particle that might enhance encapsulation.

In conclusion, the virus trap set in the blood protein nanotube ensnared the infectious HBV Dane particles selectively and completely. The efficiency of removal by a single AbNT treatment reached -3.9 log order. This astonishing result will serve as a trigger to engender a new field of virus detecting and removing devices. For instance, elimination of small and nonenvelope type viruses, such as hepatitis E virus and human parvo B19 virus, using HSA nanotubes would be of tremendous medical importance. Recombinant HSA is currently manufactured on an industrial scale,¹⁶ which enables us to exploit the protein nanotubes in practical use.

■ ASSOCIATED CONTENT

S Supporting Information. Experimental section, amount of remaining HBsAg in HBV1 solution after incubation with AbNTs determined using CLIA method (Figure S1), concentration dependence of absorbed HBsAg (HBV1) in AbNTs (Figure S2), and TEM of AbNT incorporating DPs (Figure S3). This material is available free of charge via the Internet at <http://pubs.acs.org>.

■ AUTHOR INFORMATION

Corresponding Author

komatsu@kc.chuo-u.ac.jp

■ ACKNOWLEDGMENT

This work was supported by a Grant-in-Aid for Scientific Research on Innovative Area "Coordination Programming" (Area 2107, No. 21108013) from MEXT Japan, a Grant-in-Aid for Scientific Research (B) (No. 20350058) from JSPS, PRESTO "Control of Structure and Functions" JST, and Health Science Research Grants from MHLW. Skillful experiments on the synthesis of protein nanotubes conducted by Ms. Nao Kobayashi are gratefully acknowledged.

■ REFERENCES

- (1) (a) Shimizu, T.; Masuda, M.; Minamikawa, H. *Chem. Rev.* **2005**, *105*, 1401–1443. (b) Yui, H.; Shimidzu, Y.; Kamiya, S.; Yamashita, I.; Masuda, M.; Ito, K.; Shimizu, T. *Chem. Lett.* **2005**, *34*, 232–233. (c) Kameta, N.; Masuda, M.; Minamikawa, H.; Mishima, Y.; Yamashita, I.; Shimizu, T. *Chem. Mater.* **2007**, *19*, 3553–3560.
- (2) (a) Graveland-Bikker, J. F.; Ipsen, R.; Otte, J.; de Kruif, C. G. *Langmuir* **2004**, *20*, 6841–6846. (b) Graveland-Bikker, J. F.; Schaap, I. A. T.; Schmidt, C. F.; de Kruif, C. G. *Nano Lett.* **2006**, *6*, 616–621.
- (3) Geng, Y.; Dalhaimer, P.; Cai, S.; Tsai, R.; Tewari, M.; Minko, T.; Discher, D. E. *Nat. Nanotechnol.* **2007**, *2*, 249–255.
- (4) (a) Mitchell, D. T.; Lee, S. B.; Trofin, L.; Li, N.; Nevanen, T. K.; Söderlund, H.; Martin, C. R. *J. Am. Chem. Soc.* **2002**, *124*, 11864–11865. (b) Hou, S.; Wang, J.; Martin, C. R. *Nano Lett.* **2005**, *5*, 231–234. (c) Hillebrenner, H.; Buyukserin, F.; Stewart, J. D.; Martin, C. R. *J. Nanosci. Nanotechnol.* **2007**, *7*, 2211–2221.

- (5) Son, S. J.; Reichel, J.; He, B.; Schuchman, M.; Lee, S. B. *J. Am. Chem. Soc.* **2005**, *127*, 7316–7317.
- (6) (a) Liang, Z.; Sucha, A. S.; Yu, A.; Caruso, F. *Adv. Mater.* **2003**, *15*, 1849–1853. (b) Yu, A.; Liang, Z.; Caruso, F. *Chem. Mater.* **2005**, *17*, 171–175. (c) Wang, Y.; Angelatos, A. S.; Caruso, F. *Chem. Mater.* **2008**, *20*, 848–858.
- (7) (a) Ai, S.; Lu, G.; He, Q.; Li, J. *J. Am. Chem. Soc.* **2003**, *125*, 11140–11141. (b) He, Q.; Cui, Y.; Ai, S.; Tian, Y.; Li, J. *Curr. Opin. Colloid Interface Sci.* **2009**, *14*, 115–125.
- (8) Lee, D.; Cohen, R. E.; Rubner, M. F. *Langmuir* **2007**, *23*, 123–129.
- (9) Qu, X.; Komatsu, T. *ACS Nano* **2010**, *4*, 563–573.
- (10) (a) Kim, D. H.; Karan, P.; Göring, P.; Leclaire, J.; Caminade, A.-M.; Majoral, J.-P.; Gösele, U.; Steinhart, M.; Knoll, W. *Small* **2005**, *1*, 99–102. (b) Steinhart, M. *Adv. Polym. Sci.* **2008**, *220*, 123–187.
- (11) Lok, A. S. F.; McMahon, B. J. *Hepatology* **2001**, *34*, 1225–1241.
- (12) Bertoletti, A.; Gehring, A. J. *J. Gen. Virol.* **2006**, *87*, 1439–1449.
- (13) Maya, R.; Gershwin, M. E.; Shoenfeld, Y. *Clinic Rev. Allerg. Immunol.* **2008**, *34*, 85–102.
- (14) Knipe, D. M.; Howley, P. M.; Griffin, D. E.; Lamb, R. A.; Martin, M. A.; Roizman, B.; Straus, S. E. *Fields Virology*; Lippincott Williams & Wilkins: Philadelphia, 2007.
- (15) (a) Kato, N.; Caruso, F. *J. Phys. Chem. B* **2005**, *109*, 19604–19612. (b) Cortez, C.; Tomaskovic-Crook, E.; Johnston, A. P. R.; Scott, A. M.; Nice, E. C.; Heath, J. K.; Caruso, F. *ACS Nano* **2007**, *1*, 93–102.
- (16) Kobayashi, K. *Biologicals* **2006**, *34*, 55–59.